PROCEEDINGS OF SCIENCE

The Nonlinear Long-term X-ray Variability of Mrk 421

Dimitrios Emmanoulopoulos*
Landessternwarte Königstuhl (LSW), Königstuhl 12, D-69117, Heidelberg, Germany
E-mail: D.Emmanoulopoulos@lsw.uni-heidelberg.de

In this work, I present the results of a thorough nonlinear time series analysis study concerning the long-term variability behaviour of Mrk 421. I use all the archival data obtained by the proportional counter array (PCA) and the all-sky monitor (ASM) aboard the Rossi X-ray timing explorer (RXTE), since 1996. Linearity and stationarity tests reveal that the long-term timing properties of the system originate from a strictly nonlinear and bistable system respectively. Moreover, from the dimensionality analysis I conclude that the underlying variability process of the system consists of numerous physical parameters, each one contributing to the observed X-ray variations equivalently in a stochastic way.

Workshop on Blazar Variability across the Electromagnetic Spectrum
April 22-25, 2008
Palaiseau, France

*Speaker.

PoS(BLAZARS2008)038

Contents

1. Introduction

BL Lacertae (BL Lac) objects are known to exhibit erratic flux variations across the whole electromagnetic spectrum, ranging from years down to minutes. The nature of these variations is strictly non-periodic but it is not clear whether they are induced by the realization of a purely stochastic or deterministic underlying physical process. Additionally, it is still unclear whether these variations reflect genuine changes of the physical parameters involved in the variability mechanism (i.e. nonstationarity) or they are just the fluctuational outcome of the same red-noise process [1]. Among all the BL Lac, Mrk 421 (z=0.031) is the brightest source in X-rays and it was the first extragalactic source detected in very high energy (VHE: $>$200 GeV) range [2]. Moreover, its X-ray light curves are not affected by absorption in the vicinity of the host galaxy, since optical high resolution images of the latter do not show any indication of large amounts of absorbing material [3]. Due to these unique features, Mrk 421 has been extensively observed during the last twenty years, and its X-ray temporal properties are considered archetypal for the BL Lac class.

2. High- or Low- Dimensional Behaviour?

The main aim of this study is to characterize the temporal properties of Mrk 421 in terms of the number of physical parameters (i.e. dimensions) involved in the realization of the variability process, as they are mapped into the observed X-ray light curves. As the number of these parameters increases, the behaviour of the system shifts gradually from the deterministic description to the stochastic one. In the time series analysis context, a variability process is characterized as low-dimensional (deterministic) if this number is $\lesssim 15$ and high-dimensional (stochastic) in the opposite case.

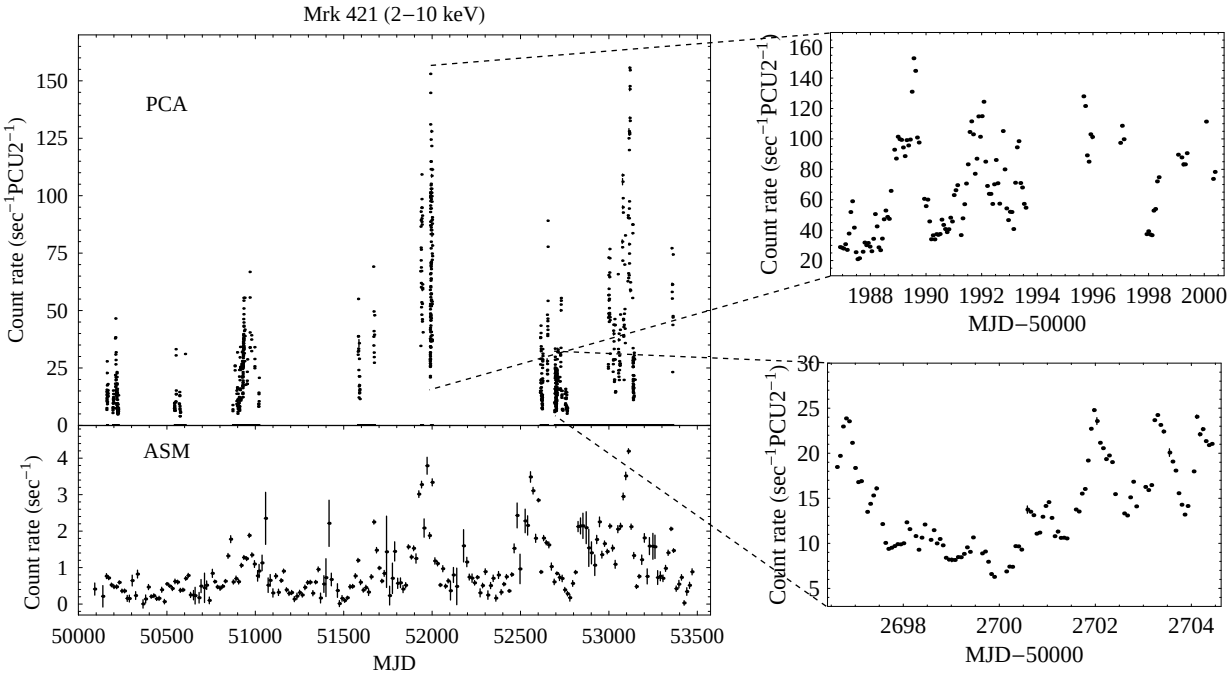

Figure 1: The long-term RXTE light curve of Mrk 421 in the energy range of 2–10 keV covering the period 1996–2004. The upper panel shows the PCA observations in bins of 5440 sec (one satellite orbit) and the two insets depict the short-term temporal properties of the source in a high and in a low activity state. The lower panel shows the ASM observations, in bins of 15 days.

3. The X-ray Data Sets

I have analyzed all the archival data of Mrk 421 in the X-ray regime (2–10 keV) obtained by the proportional counter array (PCA), aboard the Rossi X-Ray Timing Explorer (RXTE), since 1996. These observations comprise the highest time resolution X-ray data set ever been reduced homogeneously for this source. The PCA data set together with the continuous, but more sparsely sampled, observations of the all-sky monitor (ASM) aboard the RXTE, form the most extended long-term representations of the X-ray temporal properties of the source (Fig.1). Detailed description of the advanced time series analysis methods, consisting of linearity and stationarity tests, dimensionality analysis, and investigation of long-term memory behaviour, can be found in [4].

4. Results

4.1 Nonlinearity

The long-term X-ray timing properties of the source, as they are mapped into the ASM light curve, exhibit clear signs of nonlinearity. The method of *surrogate data* [5] is employed for the study of possible nonlinearities. An ensemble of 2000 artificial light curves (surrogates) is formed having the same linear properties with the ASM data set, following the methodology of [6]. Then the *correlation integral* $C_m(r_k)$ is computed based on the *delay vectors* $\vec{X}_i$ [7] for both the original and the artificial data sets (Fig.2) for m embedding dimensions, having a fixed *hyper*-sphere radius

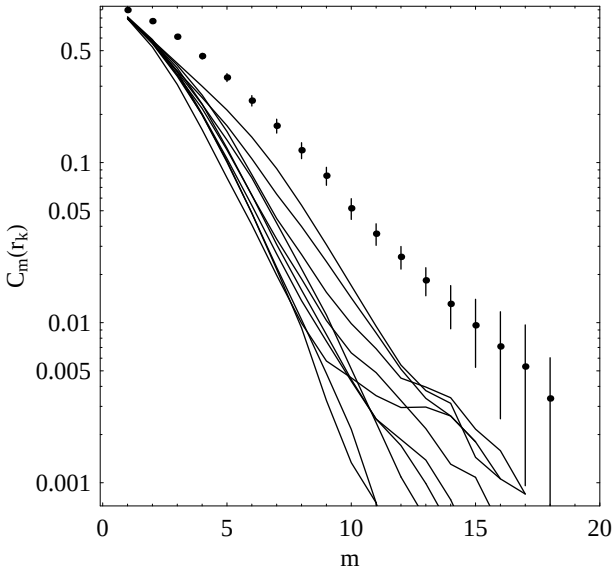

Figure 2: The value of the correlation integral (eq.4.1) of the ASM data set (black points) together with ten surrogates randomly selected from the 2000 artificial light curves (lines). The lines are used only to guide the eye among the integer values of *m*. The correlation integral is estimated for a time delay $\tau = \tau_c = 13$ bins of 15 days and for a phase radius of $r_k = 2.14$ (for the computational details see [4]).

r_k

$$C_m(r_k) = \frac{2\sum_{i=1}^{L}\sum_{j=i+1}^{L} H(r_k - \|\vec{X}_i - \vec{X}_j\|)}{L(L-1)} \tag{4.1}$$

The significant deviations of $C_m(r_k)$ between the ASM data set and its linear surrogates predicate the existence of a nonlinear variability behaviour embedded in Mrk 421.

4.2 Nonstationarity

Additionally the stationarity test reveals that the physical mechanism responsible for the observed X-ray variations of Mrk 421 consists of a process which has inherently at least two different variability states. The stationarity study has been performed by estimating the *mean value of the normalized excess variance* $\overline{\sigma_N^2}$ [8, 1] for five out of the eight observing periods (Fig.3) due to the limited number statistics. Four out of these five periods can be well fitted by the linear model $y = (2.72 \pm 0.28)10^{-4}$, having $\chi^2_{\rm red} = 0.815$ for 3 degrees of freedom (DOF) with a null hypothesis probability (NHP) of 0.49. The $\overline{\sigma_N^2}$ around MJD 51991 deviates from the linear fit ~ 7 standard deviations indicating the existence of a second variability state inherent in the source. This is the first time that such a strong evidence of nonstationarity is deduced for a BL Lac.

4.3 Dimensionality analysis

Based on the RXTE data sets and on the analysis methods, there are no robust indications pointing towards a deterministic long-term variability process in Mrk 421. The *number of physical parameters* (i.e. dimensions) involved in the realization of the underlying variability X-ray process of Mrk 421 is studied through the dimensionality analysis of the ASM data set following two methodologies.

The *correlation dimension* [9, 10] is estimated by embedding the data set into successive dimensions *m*. For each *m* the mean distance of the phase points is estimated by computing the

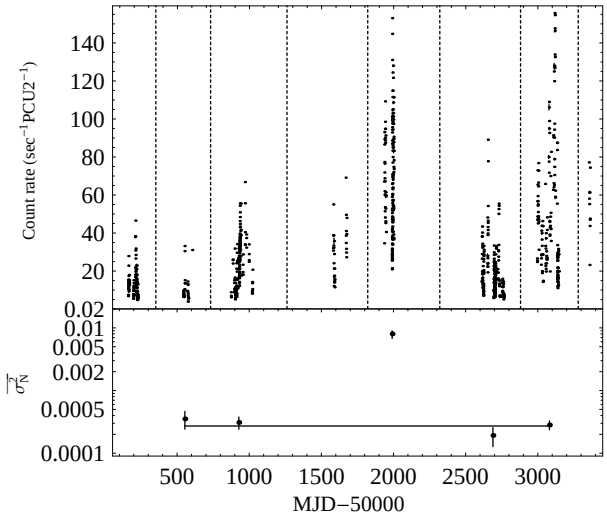

Figure 3: The upper panel shows the way that the PCA light curve (Fig.1, upper panel) has been partitioned in eight observing periods. The lower panel shows the normalized excess variance $\overline{\sigma_N^2}$ only for the five out of the eight observing periods since these are the only ones surviving the selection criteria (see [4] for details). A constant line fit for the four periods (occurring roughly at MJD 50554, MJD 50928, MJD 52689 and MJD 53081) yields $y = (2.72 \pm 0.28) \times 10^{-4}$ with $\chi^2_{\rm red} = 0.815$ for 3 DOF and NHP=0.49. The estimate for the third period around MJD 51991, is $\overline{\sigma_N^2} = 0.0080 \pm 0.0011$ and deviates from the constant line fit $\sim$7 standard deviations.

correlation integral (eq.4.1) and from that the correlation dimension $D_{2,m}$ (Fig.4, left panel). If the variability mechanism is of deterministic nature then $D_{2,m}$ should increase up to a certain dimension $(m \lesssim 15)$ and form a plateau (indicative for the noise) for larger values of m. In the opposite case of a stochastic process, no stabilization of the mean distance of the phase points is expected and therefore no plateau.

Additionally, the results of the *principal component analysis* [11, 12, 13] are shown in the right panel of Fig.4, after computing the length σ_j (singular values) of the *singular vectors* based on the *singular value decomposition* procedure for a given component j of the m dimension. Formation of a plateau at $j_{\rm pl} \lesssim 15$ indicates the existence of a deterministic variability mechanism driven from $m - j_{\rm pl}$ physical parameters.

The outcomes of both analysis methods are in accordance and consistent with a high dimensional (i.e. stochastic) variability process where all the involved parameters influence to a similar extent the long-term time evolution of the source.

4.4 Modelling

Despite the nonlinear stochastic nature of the long-term variability behaviour of Mrk 421, a direct combination of the outcomes allows to form an empirical variability model describing the long-term X-ray temporal properties of the source. The basic ingredients of the model are the nonlinearity and the nonstationarity which, in the frame of a noisy process, give raise to an intermittent bistable variable behaviour.

An empirical variability model is constructed by fitting all the observed temporal properties of Mrk 421, i.e. nonlinearity, nonstationarity and stochasticity. The existence of at least two variability states in Mrk 421, with the higher one occurring less often than the lower one, implies the existence of at least two different variability configurations in the source. Therefore an asymmetric double-well energy configuration (eq.4.2), shown in the inset of Fig.5 having minima M_1 and M_2 (i.e. the

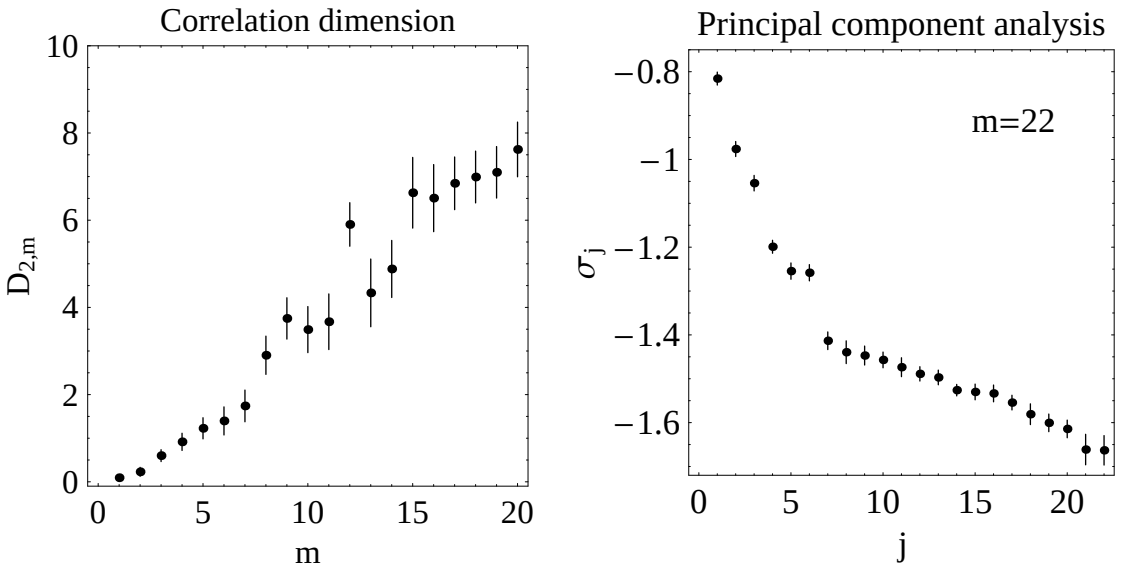

Figure 4: The left panel shows the correlation dimension $D_{2,m}$ as a function of the embedding dimension m. The right panel shows the logarithm of the normalized singular values σ_j for $m = 22$. The absence of a plateau in both plots, reveals the numerous parameters affecting the time evolution of Mrk 421 (see [4] for the power and the limitations of these methodologies).

most probable states) the mean values of the quiescent and the high activity stages respectively, is a plausible scenario

$$V(x(t)) = 0.001x(t)^4 - 0.205x(t)^3 + 14.5x(t)^2 - 401.5x(t) + 4410 \tag{4.2}$$

The time evolution of the bistable system (Fig.5) is described by

$$\frac{dx(t)}{dt} = -\frac{dV(x(t))}{dt} + 1.5r(t) \tag{4.3}$$

where $r(t)$ is a red noise component [6], constructed based on the PCA light curve (Fig.1, upper panel), having a variance of 11 counts sec^{-1} and a power spectral density slope of $\alpha = 1.65 \pm 0.15$.

References

[1] S. Vaughan, R. Edelson, R. S. Warwick, and P. Uttley. *On characterizing the variability properties of X-ray light curves from active galaxies*, *MNRAS*, **345**:1271–1284, November 2003.

[2] M. Punch, C. W. Akerlof, M. F. Cawley, M. Chantell, D. J. Fegan, S. Fennell, J. A. Gaidos, J. Hagan, A. M. Hillas, Y. Jiang, A. D. Kerrick, R. C. Lamb, M. A. Lawrence, D. A. Lewis, D. I. Meyer, G. Mohanty, K. S. O'Flaherty, P. T. Reynolds, A. C. Rovero, M. S. Schubnell, G. Sembroski, T. C. Weekes, and C. Wilson. *Detection of TeV photons from the active galaxy Markarian 421*, *Nature*, **358**:477–+, August 1992.

[3] R. Falomo, R. Scarpa, A. Treves, and C. M. Urry. *The Hubble Space Telescope Survey of BL Lacertae Objects. III. Morphological Properties of Low-Redshift Host Galaxies*, *ApJ*, **542**:731–739, October 2000.

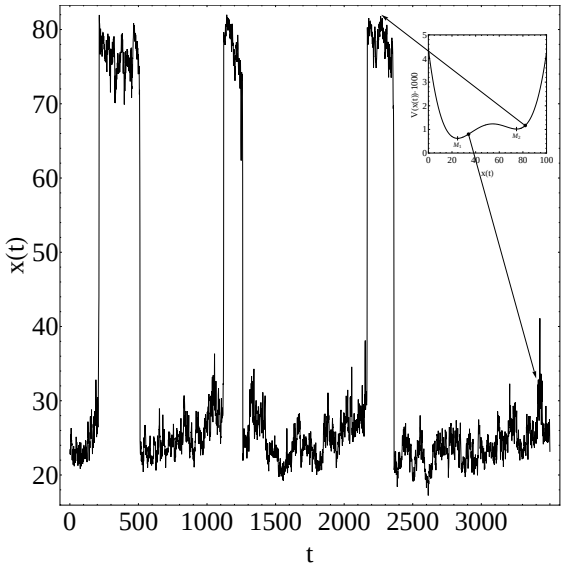

Figure 5: Time series derived from the solution of eq.4.3 for 3500 time units. The inset shows the energy state of the source $V(x(t))$ (eq.4.2) having two minima at $M_1 \simeq 24.7$ and $M_2 \simeq 74.6$. The arrows indicate the energy state of the source in two different variability levels.

[4] D. Emmanoulopoulos and S. J. Wagner. *Nonlinear Time Series Analysis Methods: An application to the long-term X-ray variability properties of Mrk 421, submitted to A&A*, 2008.

[5] J. Theiler, S. Eubank, A. Longtin, B. Galdrikian, and J. Doyne Farmer. *Testing for nonlinearity in time series: the method of surrogate data, Physica D: Nonlinear Phenomena*, **58**:77–94, September 1992.

[6] J. Timmer and M. Koenig. *On generating power law noise, A&A*, **300**:707–+, August 1995.

[7] N. H. Packard, J. P. Crutchfield, J. D. Farmer, and R. S. Shaw. *Geometry from a Time Series*, *Phys. Rev. Lett.*, **45** (9):712–716, September 1980.

[8] K. Nandra, I. M. George, R. F. Mushotzky, T. J. Turner, and T. Yaqoob. *ASCA Observations of Seyfert 1 Galaxies. I. Data Analysis, Imaging, and Timing, ApJ*, **476**:70–+, February 1997.

[9] P. Grassberger and I. Procaccia. *Characterization of Strange Attractors, Phys. Rev. Lett.*, **50** (5):346–349, January 1983.

[10] P. Grassberger and I. Procaccia. *Measuring the strangeness of strange attractors, Physica D: Nonlinear Phenomena*, **9** (1-2):189–208, October 1983.

[11] M. Bertero and E. R. Pike. *Resolution in diffraction-limited imaging, a singular value analysis I. The case of coherent illumination, Optica Acta*, **29** (6):727–746, June 1982.

[12] D. S. Broomhead and G. P. King. *Extracting qualitative dynamics from experimental data, Physica D: Nonlinear Phenomena*, **20** (2-3):217–236, June 1986.

[13] R. Vautard, P. Yiou, and M. Ghil. *Singular-spectrum analysis: A toolkit for short, noisy chaotic signals, Physica D: Nonlinear Phenomena*, **58** (1-4):95–126, September 1992.